THESIS FOR THE DEGREE OF DOCTOR OF PHILOSOPHY

Continuum modelling of particle flows in high shear granulation

PER ABRAHAMSSON

Chemical Engineering
Department of Chemistry and Chemical Engineering
CHALMERS UNIVERSITY OF TECHNOLOGY
Göteborg, Sweden 2015

Continuum modelling of particle flows in high shear granulation
PER ABRAHAMSSON

Doktorsavhandling vid Chalmers tekniska högskola
ISBN 978-91-7597-184-1
ISSN 0346-718X
Serie nr 3865

Chemical engineering
Department of Chemistry and Chemical Engineering
Chalmers University of Technology
SE-412 96 Göteborg
Sweden
Telephone: +46(0)31-7721000

Cover:
The colourful ring is the Couette shear cell used in Papers III, V and VII. In side is a sketch of a MiPro high shear granulator.

Chalmers Reproservice
Göteborg, Sweden 2015

Abstract

High shear granulation is an important process in the pharmaceutical industry. The aim of the process is to produce granules with specific properties, like size and hardness, from powder mixtures. The properties of the granules are determined by the flow field in the mixer. The most common approach taken to modelling the flow in a mixer includes tracking the forces on each individual particle and resolving each occurring collision. This gives detailed information, but the computational cost restricts this use to small-scale equipment.

Continuum modelling of particle flows means that averages are made to form a continuous flow rather than tracking individual entities. The problem that arises in this procedure is correctly describing the transfer rates of mass and momentum in the system. The focus of the research in this thesis is on evaluating previously used continuum models, and finding and developing new approaches. The connection between flow field information and the evolution of particle properties is also studied through the development of a compartment model.

Results show that the continuum model currently being used has a promising parameterization for describing the overall effect on a flow field caused by particle property changes that occur during granulation. The model is; however, not capable of adequately resolving the flow field in the important regions close to the walls and the impeller of the vessel where the particle volume fraction is high. A rheology-like model is used to improve the dense granular flow regions, while the theory for the more dilute parts is improved via kinetic theory models modified for inelasticity and improved for its validity in the transition region to dense flows.

Keywords: High shear granulation, continuum modelling, granular flow, parameter study, resolution dependence, kinetic theory of granular flow, compartment model

List of papers

This thesis is based on the following enclosed papers:

Paper I **Parameter study of a kinetic-frictional continuum model of a disk impeller high-shear granulator**
Abrahamsson, P.J., Niklasson Björn, I. and Rasmuson, A.
Presented at the 9th International Symposium on Agglomeration
Powder Technology (0032-5910). Vol. 238 (2013), p. 20-26.

Paper II **The rheology of dense granular flows in a disc impeller high shear granulator**
Khaliliteherani, M., Abrahamsson, P. J., Rasmuson, A.
Powder Technology (0032-5910). Vol. 249 (2013), p. 309-315.

Paper III **On continuum modelling using kinetic-frictional models in high shear granulation**
Abrahamsson, P. J.,Sasic, S. and Rasmuson, A.
Particuology (1674-2001). Vol. 13 (2014), p. 124-127.

Paper IV **Modeling dilute and dense granular flows in a high shear granulator**
Khaliliteherani, M., Abrahamsson, P. J., Rasmuson, A.
Powder Technology (0032-5910). Vol. 263 (2014), p. 45-49.

Paper V **On the continuum modelling of dense granular flow in high shear granulation**
Abrahamsson, P. J.,Sasic, S. and Rasmuson, A.
Powder Technology (0032-5910). Vol. 268 (2014), p. 339-346.

Paper VI **Analysis of meso-scale effects in high shear granulation through a CFD-PBM coupled compartment model.**
Abrahamsson, P. J., Kvist, P., Yu, X., Reynolds, G., Björn Niklasson, I., Rasmuson, A.
Manuscript

Paper VII **Continuum modelling of dense and inelastic particle flows in high shear granulation.**
Abrahamsson, P., Sasic, S., Rasmuson, A
Manuscript

Contribution report

Paper I Main author. Performed and planned all simulations, interpreted the results.

Paper II Active in the planning and execution of all experiments and simulations. Took part in the interpretation of the results.

Paper III Main author. Performed and planned all simulations, interpreted the results.

Paper IV Active in the planning and execution of all experiments and simulations. Took part in the interpretation of the results.

Paper V Main author. Performed and planned all simulations, interpreted the results.

Paper VI One of the main authors. Active in the planning and execution of the CFD simulations and the development of the compartment model. Not part of the development of the PBM solver code that was used. Active in the analysis and interpretation of the results.

Paper VII Main author. Performed and planned all simulations, interpreted the results.

Acknowledgments

First, I would like to thank my supervisor Professor Anders Rasmuson for his support, encouragement and for always taking time to help out.

Second, I would like to thank my assistant supervisors Doctor Ingela Niklasson Björn at Astra Zeneca and Professor Srdjan Sasic at the Department of Applied Mechanics for their help with practical and theoretical matters.

I would also like to thank:

Astra Zeneca for financing this project.

Mohammad Khaliliteherani for great cooperation.

Dr. Gavin Reynolds, Dr.Xi Yu and Professor Mike Hounslow for good discussions and cooperation on Paper VI.

Jan Emnér and Lars-Göran Johannesson.

Patric Kvist and Simon Lundevall for doing their M.Sc. thesis under my supervision. Great work!

My father for reading the manuscript and giving linguistic support.

My roommate Matthias Eng for all the relevant and irrelevant discussions we had.

All my colleagues and former colleagues at Chemical Engineering for always making my workday fun.

Family and friends for all your support.

Finally, I would like to thank my lovely wife Julia and our wonderful kids Linus and Ella, thank you for always supporting me and making me happy! I love you!

Table of Contents

1. Introduction

High shear granulation is a common process in the pharmaceutical industry. The process consists of three steps: dry mixing, where powder ingredients are mixed; liquid addition, where a binder liquid is added and agglomeration starts; and wet massing, where granules are processed to the desired properties in the shear field of the mixer. The process is used to ensure the homogeneous mixture of tablet ingredients and to improve the flow and process ability of the material.

Mathematical models are of great importance for predicting granulate properties such as size distribution, particle density distribution and particle liquid content distribution. Population balance equations have been developed to describe the evolution of these properties [Darelius et.al. 2006, Niklasson Björn et.al. 2005, Hounslow 2001]. The rate of property changes is described in so called kernels, and is determined by the flow conditions in the equipment. The flow information can be incorporated into the kernels either from experimental measurements or through flow field modelling [Gantt et.al 2006a]. The flow situation in a high shear granulator is one in which the volume fraction of solids approaches close packing and high shear rates near the impeller, while the flow in the bulk of the vessel is dispersed [Ng et.al. 2007]. Nevertheless, the kernels are normally based on the assumption of a homogeneous system with a global rate of change of particle properties [Iveson et.al. 2001]. To develop improved models for high shear granulation, more information about the flow conditions in a mixer is needed [Iveson et.al. 2001].

The most common approach to modelling the flow conditions in granulators is currently Discrete Element Modelling (DEM). A review of the use of DEM in the pharmaceutical industry is given in [Ketterhagen et.al. 2009]. Other examples of its use in high shear mixing, specifically, are [Gantt et.al. 2006a] and [Gantt et.al. 2006b]. In the DEM approach, momentum balances are put up and solved for all particles individually. This yields a detailed model that takes into account the forces that act on each individual particle. One drawback is computational cost, the result of which is that only small-scale systems (1 000 000 particles [Ketterhagen et.al. 2001]) can be modelled. If large-scale equipment is to be modelled, for studying the effects of process scale-up, a different approach is needed.

Continuum descriptions of granular flows have been used since the pioneering work of Bagnold [Bagnold 1954] and are common in flow field modelling of other particle processes, both industrial and natural, like fluidized beds [van Wachem et.al. 1998, van Wachem et.al. 1999, Passalacqua et.al. 2009] or land slide and avalanche motion

[McDougal and Oldrich 2004]. Continuum descriptions have only recently been introduced to the study of high shear granulation [Darelius et.al. 2008] and [Ng et.al 2009]. The continuum treatment of the granular phase of the process allows for the potential to model systems with a larger amount of particles than is possible with DEM. The approach used for continuum modelling, in the two mentioned papers, is based on an averaging procedure of particle motion. The procedure is similar to that used in kinetic gas theory, with attention given to drag forces between air and the particle phase, inelastic collisions and added frictional stresses in the regions with a high volume fraction of solids. In [Darelius et.al. 2008] and [Ng et.al. 2009] it was concluded that there are discrepancies in the model predictions for the parts with a high volume fraction of granules; near the walls of the vessel and the impeller blades. The reasons for the discrepancies have not been fully examined, and further studies using the same modelling framework on simpler high shear granulation equipment would be beneficial for deciding how to improve the models. There are also other approaches to modelling granular flows with high volume fractions available and used in other fields. Investigating and evaluating their potential use for modelling high shear granulation could be a major step forward for flow field modelling and the scale-up of equipment.

1.1. Objectives

The purpose of this research is to develop a continuum model suitable for modelling high shear granulation systems. This would be extremely useful for the purpose of equipment scale-up since both small-scale and large-scale processes could then be modelled. The research started with further evaluation of the already used framework of the kinetic theory of granular flow with added frictional stress. There are other concepts available from other areas in which particle flows occur, and the research has progressed with an investigation of other promising concepts, such as kinetic theory models made for flows of high volume fractions with inelastic particles and empirical approaches of a rheological nature. In addition to the evaluation of continuum models, attention has also been directed towards the connection to the modelling of particle properties through population balance equations.

1.2. Outline of the thesis

The next chapter describes high shear granulation in order to obtain an understanding of the flow situation in a mixer. Chapter three then describes the physics in granular flows, focusing on the different flow regimes present in a mixer. Chapter four briefly introduces the experimental techniques used in two of the articles. Chapter five gives the current situation in continuum phase modelling in high shear granulation. Chapter six evaluates the models described in the previous chapter and discusses available improvements to the modelling framework. Chapter seven discusses the coupling to population balance models. Chapter eight discusses the results and nine concludes the discussion. Future research is briefly discussed in the last chapter.

2. High shear granulation

The following section will describe the conditions in a general granulator under the three stages of powder mixing, liquid addition and wet massing, consecutively. The focus is on powder mixing and the later part of the wet massing stages in which particle contacts can be considered to be dry contacts. This is because the models in the present research have not taken wet contacts into account. The findings can also be applied to dry high shear granulation.

The powder mixing phase consists of the mixing of dry powder ingredients. The purpose is to achieve a homogeneous mixture of the ingredients. The particles in this phase are commonly in the size range of 1 µm to 100 µm. The forces acting on each particle in the flow field are drag force from the surrounding air, collisions from other particles, frictional gliding against other particles in high volume fraction areas (as the volume fraction approaches close packing) and possible cohesive forces; depending on the material and the size of the particles.

In the liquid addition stage, a binder liquid is normally sprayed onto the powder from the top of the vessel. Droplets from the binder adhere to the powder particles, and this starts the agglomeration process. In this stage, liquid bridges are formed between particles and introduce other types of physics; however, studying these phenomena during this part of the process is beyond the aim of this project.

When the addition of liquid is stopped, the wet massing stage starts. The desired granulate properties are to be reached by using the required granulation time, impeller and chopper speeds. System properties change as size distribution is driven towards larger particles and the granules are compacted in the shear field. The liquid becomes more and more encapsulated in the forming granules, and the physics of the flow once again start to resemble the physics in the powder mixing phase, although the properties of the particles have changed.

There are different types of high shear granulator devices, and three examples that will be mentioned further in this thesis are the MiPro mixer, the vertical high shear mixer, the Diosna mixer and the disc impeller granulator.

The MiPro and Diosna mixers consist of a three-bladed impeller mounted from the top for the MiPro and from the bottom for the Diosna. Figure 2.1 shows a lab-scale Mipro device.

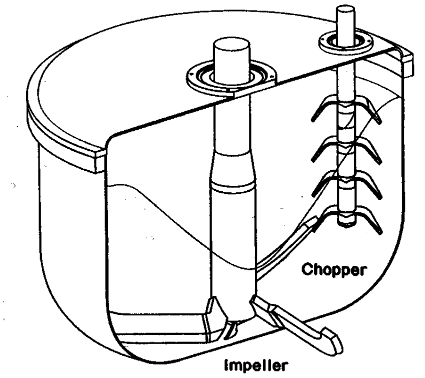

Figure 2.1. A MiPro high shear granulator.

The MiPro system also contains a second small-bladed chopper mounted at the top of the vessel designed to break large particle aggregates.

A vertical high shear mixer consists of several blades mounted at different heights in a tube-like vessel. Figure 2.2 shows a sketch of a vertical high shear mixer.

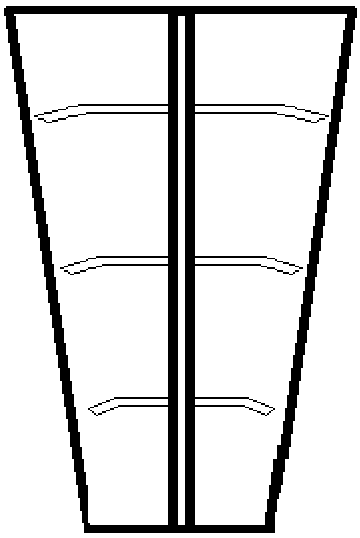

Figure 2.2. A sketch of a vertical high shear mixer with three mounted blade pairs.

A disk impeller high shear granulator is basically a vessel with a flat rotating bottom plate. The system is used as a model system with a simpler geometry while retaining the dense sheared part of the flow field.

2.1 The flow situation in a high shear mixer

The flow situation in a high shear mixer is complicated. It is a three-phase system of liquid droplets, solid particles and gas. It is a multi-body system with non-trivial interactions between the particles, and there are sharp gradients in both the velocity and volume fraction in the system. Momentum transfer can take place through a translation of particles or a collision between particles. Collisions can be binary or multi-body, and they can be instantaneous or long duration contacts with or without frictional gliding.

The characteristics of the particle flow in high shear mixers have been experimentally studied in [Ng et.al 2007 and Knight et.al. 2001]. It was concluded there that the bulk region of the flow belongs to the so-called rapid granular flow regime, where the momentum transfer is dominated by a translation of particles and binary particle collisions. Close to the impeller and the walls of the vessel, the flow has a radically different character in which the high volume fractions of solid particles in combination with shear forces create considerable frictional particle interactions [Ng et.al 2007 and Knigth et.al. 2001]. These regions have proven to be of great importance for the flow inside high-shear mixers [Darelius et.al. 2008] [Ng et.al. 2009], and have also been shown to be the most problematic to describe with continuum models. There are reliable models for rapid regime flows, as will be described below, and the focus in this thesis will, consequently, be on high solid volume fraction flows in the transitional and dense regions.

3. Physics of granular flow

The physics of granular flows are versatile and dependent on the regime of a flow. Granular flows are typically divided into quasi-static and rapid regimes. A quasi-static flow occurs; for example, on the slope of a pile of particles, or as particles pour down a hopper. This flow is characterized by long duration particle contacts and frictional interaction. A rapid regime flow is encountered; for example, in fluidized beds and is a state in which individual granules freely fly around with only brief binary interactions with one another. Figure 3.1 summarizes some properties of the two regions.

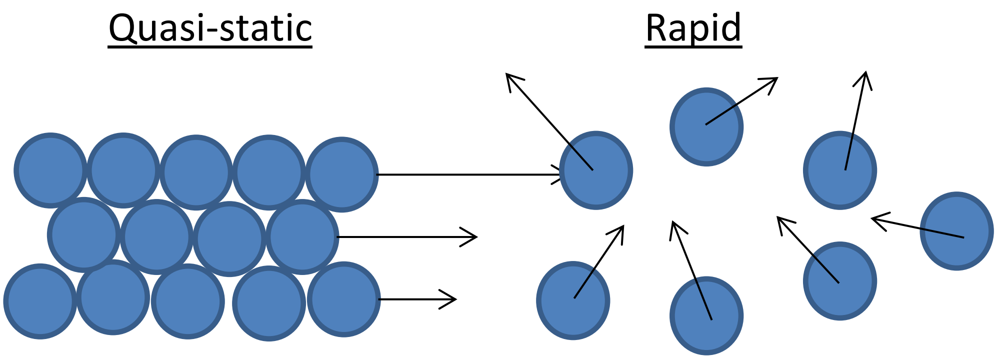

	Quasi-static	Rapid
Behaviour:	Solid-like	Fluid-like
Rheology:	Plastic	Viscous
Mechanisms for transfer:	Friction	Binary Collisions

Figure 3.1. Properties of the two regimes of granular flow

Figure 3.1 shows the behaviour of two states of granular flow as solid-like and fluid-like. Solid-like behaviour occurs when the particles have collective behaviour. The motion of the particles is correlated to some length scale longer than particle diameter [Mueth 2003]. Sheets of particles sliding over each other, as in the figure, is one example, and particle clusters tumbling around is another. The rapid regime is described as a fluid-like state, which means that the properties of the flow are locally determined. In the quasi-static flow regime, dissipative frictional interactions make the behaviour plastic in the sense that stresses in the material have no strain-rate dependence. This is in contrast to flow in the rapid regime which displays a quadratic stress-strain relationship. The differences in rheological behaviour stem from the different mechanisms for the two flow types. In a quasi-static flow the main mechanism is frictional interactions. Frictional gliding can be well described by the Coulomb law of friction which is strain-rate dependent [Coulomb 1776]. In contrast, the momentum transfer in the rapid regime is governed by particle translation and binary particle collisions. The rate of the translation and collisions of particles is determined by particle velocity fluctuations around the mean flow velocity. This is because, in a shear field, this property will be the reason for particles of one mean velocity to either collide with a particle with a different mean velocity, or move into a region with a different mean velocity. These velocity fluctuations in the fluid-like state are analogous to the temperature of a molecular fluid, and are often called the granular temperature, defined as Equation 3.1.

$$T = \frac{1}{3}\left\langle C^2 \right\rangle \qquad \text{Eq.3.1}$$

Granular flows in high-shear mixers include both of these regimes, as stated in the previous chapter. This leads to regions in which the flow situation is a mixture of the two conditions. Such a mixed condition has not yet been well described rheologically, and the limits for when each model is applicable have not been fully determined either.

To study the behaviours of granular flows, model systems are often used for experimental studies of sheared granular flows at high solid volume fractions [GDR MiDi 2004]. A suitable system for investigating the dynamics of such systems is the Couette shear cell. Bagnold studied the rheology of suspended spherical wax particles, 1.3mm in diameter, in a Couette configuration in 1954 [Bagnold 1954]. The experiments showed a quadratic relation between stress and strain in the rapid granular flow regime. This observation implies that the momentum transfer in the granular media is determined by binary instantaneous collisions. When the solid volume fraction approaches close packing, the nature of the particle interaction changes towards the existence of long duration contacts with possible frictional interactions. Frictional interactions are well described by the Coulomb friction law [Coulomb 1776], which is rate-independent. Savage and Sayed 1984 [Savage and Sayed 1984] have shown that the dependence of shear rate on strain rate moves towards a rate-independent relation when the solid volume fraction is increased above 0.5, at low shear rates, when spherical glass beads, 1.8 mm diameter, are sheared in a Couette device. By studying the flow of walnut shell pieces, the same authors were able to show that the deviation from the rapid flow regime starts at different values of the solid volume fraction depending on the frictional properties of the material. As the solid volume fraction approaches that of the close packing of spheres, there is a change in the behaviour of the system from fluid-like, where transport properties are dependent on local conditions, to solid-like behaviour where particles exhibit collective behaviour. This was observed by Mueth 2003 [Mueth

2003] who found both spatial and temporal correlations in particle movements at volume approaching close packing. When the solids volume fraction is increased further, there is no longer a flow of individual granules, but rather the packed granules exhibit solid-like behaviour. The conditions for when the transition between these states start have not been clearly determined, and neither has the rate of change in the transport properties as the system progresses towards a purely frictional behaviour. Hsiau and Shien 2000 [Hsiau and Shien 2000] have studied the influence of the solid volume fraction on the flow of glass spheres in a Couette device, and found a strong dependence of the velocity profile on small changes in the volume fraction when the latter is above 0.53. The rate of the divergence of the momentum transfer remains to be determined.

In the rapid flow regime, where momentum transfer is governed by particle collisions, the velocity fluctuations around the mean particle velocity determine the rate of collisions in the flow. The behaviour of the velocity fluctuations at high solid volume fractions has been studied in Couette devices by; for example, [Hsiau and Shien 2000] [Bocquet et.al. 2001]. These authors found that in sheared flows of a high solid volume fraction, the fluctuations in the flow direction show a relative increase [Hsiau and Shien 2000], whereas the velocity fluctuations in dilute particle flows with small velocity gradients are isotropic. Bouquet et. al. 2001 [Bouquet et. al. 2001] have found that velocity fluctuations decay slower than the average motion of particles as the solid volume fraction approaches close packing. The difference in the rate of divergence of the rate of momentum and the velocity fluctuations is important in the transition between solid-like and fluid-like behaviour. This statement will be further addressed below.

An important discussion has focussed on the clustering and stability of rapid granular flows in fluidized beds, where dilute to intermediate volume fractions are treated, and where drag is of large importance[Agrawal et.al. 2001]. This is also of importance in the more dilute regions of a high shear granulator. The reasons for the clustering can be attributed to either drag interaction between the phases, the resolution used in the numerical simulations or the inelasticity of particle collisions [Agrawal et.al. 2001] [Mirtano et.al. 2014]. This effect is important in order to resolve meso-scale flow structures in the dilute to intermediate phase in a high shear granulator.

In brief, the properties that are being sought for in a model for high shear granulation are: a model that is able to describe the transition between fluid-like and solid-like behaviour which means that the rates of divergence of momentum transfer and velocity fluctuations must be determined. This transition should be dependent on the frictional properties of the material. A model should also be able to predict the anisotropy of fluctuating velocity in a sheared system and the formation of meso-scale clusters in inelastic particle flows.

4. Experimental techniques

In this research, high speed camera imaging was used in Papers II and IV combined with Particle Image Velocimetry (PIV) to validate the surface velocities of the model used in the disk impeller system. In this chapter, a short description of the technique and the equipment will be given.

4.1 Equipment

The system used for the measurements was a Plexiglas disc impeller system with a diameter of 7.2cm. The system is similar to those used in Knight et.al. [Knight et.al. 2001], and was chosen for its simple geometry and presumed dense sheared flow. The system is shown in Figure 4.1 in which the camera setup is also shown. The particles used for the experiments were 1.3mm glass particles sieved to a precision of ± 0.05 mm. The choice of particles was dependent on the availability of data for the parameters in the rheology model. The motor for the impeller was mounted to a dynamometer that held it in place and measured the force needed to keep it in place, which corresponds to the force input to the impeller.

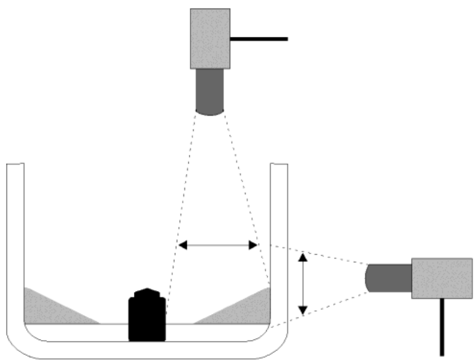

Figure 4.1. The disc impeller system used in Papers II and IV.

4.2 High speed camera and PIV

The high speed camera used was set to an imaging rate of 500 fps with a resolution of 240 times 512 pixels. The pictures were paired up in Matlab to allow for calculations of the particle displacement between each pair using the PIV software DaVis 6 by LaVision. The PIV analysis was conducted with a so called multi-pass method with interrogation window sizes ranging from 32 times 32 to 64 times 64 pixels. The pixels were determined to correspond to 0.13mm in the pictures, giving approximately 10 to 40 particles per interrogation window. This size is considered to give a good representation of the mean field velocity, and enables finding regions with velocity fluctuations, although it cannot resolve individual particle motion. Averages were then made over a picture sequence of 2s for the mean field velocities, and the standard deviation of the velocities was used to find fluctuating regions.

5. Continuum modelling of granular flow

Continuum modelling of particle flows is built on an averaging procedure in which the transport of discrete entities is translated into a continuous medium. Three different forms of averages are considered here; volume average, time average and ensemble average. Ensemble average is an average based on the measurements from several independent realizations of the same property. The use of an ensemble average is unrestricted, but the formation of it is restricted to uncorrelated measurements. Time and volume averages can, in contrast, be formed in all systems. The use of volume and time averages is restricted in the sense that they provide relevant information to systems in which there is a separation of scales [Enwald et.al. 1996]. Separation of scales means that the characteristic time and length scales of the particles in a flow are much smaller than the characteristic time and length scales of the flow. Figure 5.1 shows a representation of an average value as the averaging interval, time or volume, is increased.

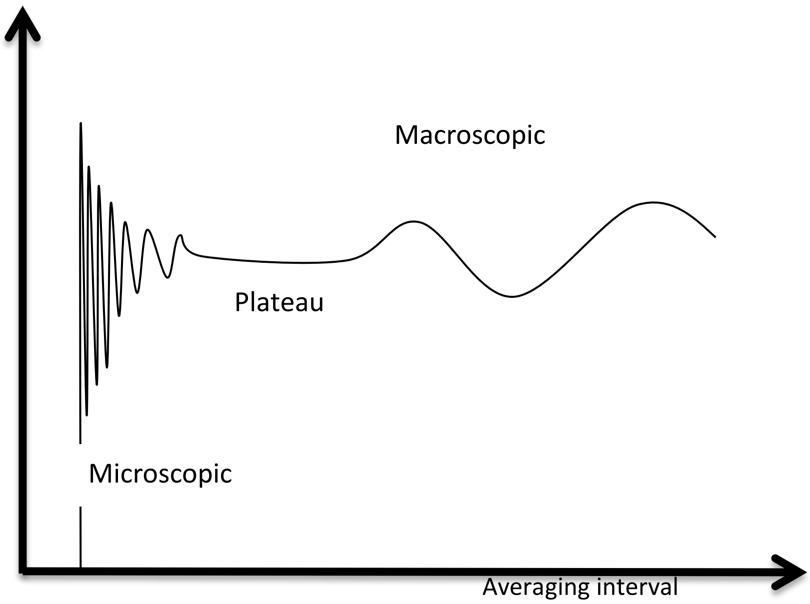

Figure 5.1. A representation of a measured average as the size of the measured interval is increased, in a system with a separation of microscopic and macroscopic flow scales.

When the averaging interval is smaller than the particles characteristic property, the mean will be based on whether or not a particle is present in the measurement. The microscopic properties of the system dominate the measurement. This is seen as the first part of the graph in Figure 5.1 in which the value starts at zero and jumps to the value of the first particle. This jumping behaviour continues as long as the action of single particles entering or leaving the measurement has a strong influence on the mean value. Eventually, if there is a separation of scales, there will be a plateau of the mean value that will well represent the state of the system. Increasing the interval further will lead to the inclusion of regions with different macroscopic properties. To resolve macroscopic fluctuations, the averaging interval needs to be smaller than the scale of the macroscopic fluctuations.

Molecular flows usually have a clear separation of scales. This is, in general, not so clear in granular flows. This difference between molecular systems and granular systems stems not only from the size of the entities, but also from the difference in that granular systems are dissipative through their inelastic particle collisions [Glasser and Goldhirsch 2001]. This can be seen in an analysis of flow scales as done in [Glasser and Goldhirsch 2001]. In condensed form, the analysis starts with the so called equation of state for rapid granular flows, Equation 5.1.

$$T = C\frac{\gamma^2 l^2}{\epsilon}. \qquad \text{Eq.5.1}$$

Where T is the granular temperature, l is the mean free path, γ is the shear rate, $\boldsymbol{\epsilon}$ is the inelasticity (ranging from 0 = elastic to 1 = inelastic) and C is a volume fraction dependent constant in the size range of unity, O(1). The time scales are also defined as in Equations 5.2 and 5.3.

$$\tau_{Micro} = \frac{l}{\sqrt{T}} \qquad \text{Eq.5.2}$$

$$\tau_{Macro} = \gamma^{-1} \qquad \text{Eq.5.3}$$

From Equation 5.1 and the notion of the microscopic and macroscopic time scales, Equation 5.4 can be derived.

$$\frac{\tau_{Micro}}{\tau_{Macro}} = \frac{\sqrt{\epsilon}}{\sqrt{C}} = O(1) \qquad \text{Eq.5.4}$$

Since C=O(1), the ratio in Equation 5.4 is also of the same order of magnitude as long as the inelasticity of the system is not much smaller than one. A similar analysis can also be made for length scales, see [Glasser and Goldhirsch 2001].

This inherent lack of scale separation in granular flows is an important feature in the modelling of these systems. The effects of the lack of separation of scales have not been considered in continuum modelling of granular flows in high shear mixers. The attached Paper II is a study of the implications of this property on sheared high solid volume fraction flows, when the frictional stress model by Shaefer [Shaefer 1987] and Johnson and Jackson [Johnson and Jackson 1987] is applied. Even if there is intrinsic scale dependence for dense granular flows, there remains much evidence that an applicable model may be found using experimentally based semi empirical models that treat dense granular flow. Bocquet et.al. 2001 [Bocquet et.al. 2001] have developed an experimentally supported modification to the shear viscosity in a Kinetic theory of granular flow framework. Jop et.al. [Jop et.al. 2006] used shut flow experiments to derive a pressure dependent modification of a Hershel-Bulkely fluid. This led to a scale independent set of equations, which were shown to be able to give relevant predictions for the material used in different flow setups [Jop et.al. 2006]. Another way is to incorporate scale dependence in the derivation of the equations. For example, in the revised Enskog theory [van Beijeren and Ernst 1979], which will be described in a following chapter, the solution is expanded around a reference state that is dependent on the local properties of the flow, and can correctly describe granular systems at equilibrium for all time and length scales [Garzo and Dufty 1999].

These approaches will be investigated in this thesis for use in high-shear granulation, and the theory behind them will be presented in Chapter 7. In the next chapter, the state of continuum models of granular flows in high shear granulation at the start of this project will be addressed.

6. Review of previous research in the field

Continuum modelling of the particle phase in high-shear granulation equipment has previously been done in [Darelius et.al 2008]and [Ng et.al 2009]. In both attempts, the same modelling framework was used; the kinetic theory of granular flow developed in [Gidaspow et.al. 1992] with the added frictional stress model developed in [Shaeffer 1987]. More details about this modelling framework will be given in Chapter 7. In [Darelius et.al 2008] a MiPro system with a three-bladed impeller was modelled during the powder mixing phase. The powder was micro crystalline cellulose with a particle diameter of 60µm. No chopper was present. The simulations were compared with velocity data extracted from a series of high-speed image photos at the vessel wall.

A comparison between the simulations and the experimental data showed that the bed height could be well predicted as well as the velocity magnitude near the wall. When the velocity was divided into its components and analysed, differences between the model and the experiments were found. Tangential motion was underestimated by the model while the axial velocity was overestimated. The model also had a general underestimation of the viscosity in the near-wall region. Some different explanations were offered by the authors: that the cohesion of the powder was not included in the model; that the partial slip boundary condition used was inadequate for dense particle flows; that the mesh resolution was inadequate near the wall; but the most probable reason was the inadequacy of the frictional stress model.

In [Ng et.al. 2009], a vertical high shear mixer was studied during the powder mixing phase with calcium carbonate particles of 60µm size. Their simulations were compared to positron emission particle tracking (PEPT) experiments. This technique follows a radioactive tracer particle inside the equipment, and, can, consequently, give a picture of the entire flow field in the equipment. It was found that this model also gave poor predictions for the distribution between the velocity components, with a general over-prediction for the tangential velocity in the bulk flow, and the simulation results predicted a decrease in the tangential velocity at the wall that was too steep. This is in accordance with the findings by [Darelius et.al. 2008]. In [Ng et.al. 2009], a no-slip boundary condition was used. The reason for this is that the boundary condition is not the only reason for the near-wall discrepancy in the model. Calcium carbonate particles are less cohesive than micro-crystalline cellulose particles. A spatial resolution dependence study was done, but only for general flow features and not specifically for the problematic near-wall region.

The conclusion was that this modelling framework showed some ability to model high-shear granulation, and further studies of the dynamics of this modelling framework would be useful. However, it was also found that the discrepancies in the spatial resolution dependence of the dense regions needed to be further studied, and if no remedy could be found, it would be useful to investigate other approaches to modelling dense granular flows as a continuum.

7. Model theory

This chapter will introduce the theory behind the models used in this research. It will begin with a general description of the KTGF models with a focus on the assumptions made in the derivation. This will be followed by descriptions of the alternative models applied in the attached articles.

7.1 Kinetic theory of granular flow

To define a particle system, the positions and velocities of all particles need to be known. These can be described with a probability function which pinpoints the likelihood of finding a particle with a certain velocity in a certain position. The Boltzmann Equation describes the evolution in time of this so called probability density function (Equation 7.1).

$$\frac{\partial}{\partial t} f(r_1, v_1, t) + v_1 \cdot \nabla f(r_1, v_1, t) + \frac{\partial F f}{\partial v_1} = J_E[r_1, v_1, f(t)] \qquad \text{Eq.7.1}$$

The changes in the distribution are assumed to come from three phenomena; the translation of particles (described by the second term), the external forces acting on the particles (described by the third term) and the collisions between particles (described by the last term). In [Gidaspow et.al. 1992] the external forces included were gravity, buoyancy and drag forces from the surrounding gas.

In order to obtain an expression for the collision term, $J_E[r_1, v_1, f(t)]$, the conditions for the particle-particle interactions must be determined. In the KTGF, it is assumed that all collisions are binary and instantaneous. This assumption implies that the system is dilute, since the occurrence of multi-body contacts is neglected. It also implies that the particles are hard, meaning that there is no deformation of the particles during a collision since that would imply that the collisions are not instantaneous. The collisions are elastic or allowed to be slightly inelastic, meaning that only a small fraction of the kinetic energy is lost. With these assumptions, an expression for the collisional contribution to the change in the probability density function can be written as Equation 7.2.

$$J_E[\boldsymbol{r_1}, \boldsymbol{v_1}, f(t)] = \sigma^2 \int d\boldsymbol{v_2} \int d\boldsymbol{\hat{\sigma}} \boldsymbol{\theta}\big(\boldsymbol{\hat{\sigma}} \cdot (\boldsymbol{v_1} - \boldsymbol{v_2})\big)\big(\boldsymbol{\hat{\sigma}} \cdot (\boldsymbol{v_1} - \boldsymbol{v_2})\big) \times \big\{e^{-2} f^{(2)}\big(\boldsymbol{r_1}, \boldsymbol{r_1} - \boldsymbol{\sigma}, \boldsymbol{v_1'}, \boldsymbol{v_2'}, t\big) - f^{(2)}(\boldsymbol{r_1}, \boldsymbol{r_1} + \boldsymbol{\sigma}, \boldsymbol{v_1}, \boldsymbol{v_2}, t)\big\} \qquad \text{Eq.7.2}$$

Where $f^{(2)}$ is the pair particle distribution function, the distribution of particle pairs with the properties needed for a collision. e is the restitution coefficient and **v'** is the precollisional velocity and **v** is the post collisional velocity related through the relation $\boldsymbol{v} = \boldsymbol{v} \pm \frac{1}{2}(1 + e^{-1})\big(\widehat{\boldsymbol{\sigma}} \cdot (\boldsymbol{v_1} - \boldsymbol{v_2})\big)\widehat{\boldsymbol{\sigma}}$.

Assuming that the properties of each single particle in each particle pair are uncorrelated to the properties of the other particle, the pair particle distribution function can be written as the product of the individual particle distribution functions Equation 7.3. This is called the assumption of molecular chaos [Jeans 1962].

$$f^{(2)}(\boldsymbol{r_1}, \boldsymbol{r_2}, \boldsymbol{v_1}, \boldsymbol{v_2}) \approx g_0(\boldsymbol{r_1}, \boldsymbol{r_2}, n(t)) f(\boldsymbol{r_1}, \boldsymbol{v_1}, t) f(\boldsymbol{r_1}, \boldsymbol{v_1}, t) \quad \text{Eq.7.3}$$

To adjust for the fact that the particles have a volume, and, consequently, a larger probability of colliding, a function is introduced $g_0(\boldsymbol{r_1}, \boldsymbol{r_2}, n(t))$. It is called the equilibrium radial distribution function in which $n(t)$ is the non-equilibrium density function defined by $n(t) = \int d\boldsymbol{v} f(\boldsymbol{r}, \boldsymbol{v}, t)$. The equilibrium radial distribution function describes the system from the perspective of the single particle in relation to the experienced available space. This decreases the amount of possible configurations due to the volume occupied by other particles. It contains strong volume fraction dependence and the function chosen depends on the regime of flow [Luding 2009]. Luding [Luding 2009] reviews a number of functions used for 2D systems showing the diversity of expressions available.

7.1.1 The transport equations

Solving the full Boltzmann Equation is possible but not trivial. Instead, it can be sufficient to find a solution that preserves the properties of interest in the system. In such a case, the first three statistical moments of the Boltzmann Equation are typically considered. They represent mass, momentum and fluctuating kinetic energy (or granular temperature). In this step, it is assumed that ensemble averaging can be applied, or, if not, large time averages can be used, but then the small time scale dynamics will be lost. The equations are presented in the same form as in [Gidaspow et.al. 1992] in Equations 7.4-7.6.

$$\frac{\partial}{\partial t}(\alpha_s \rho_s) + \nabla(\alpha_s \rho_s v_i) = 0 \qquad \text{Eq.7.4}$$

$$\frac{\partial}{\partial t}(\alpha_s \rho_s v_i) + \nabla\big(\alpha_s \rho_s v_i v_j\big) =$$

$$-\alpha_s \frac{\partial p}{\partial x_i} + \alpha_s \rho_s g_i + \beta(u_i - v_i) + \frac{\partial}{\partial x_j}\big(\tau_{ij}^k + \tau_{ij}^c\big) \qquad \text{Eq.7.5}$$

Where β is the drag coefficient and τ_{ij}^{k} and τ_{ij}^{c} are the kinetic and collisional contributions to the stress tensor. The subscripts denote if the bulk solid phase is considered, x_s, or if it is the property of a single particle, x_p.

$$\left[\frac{\partial}{\partial t}\left(\alpha_s \rho_p \frac{\langle C^2 \rangle}{2}\right) + \nabla\left(\alpha_s \rho_p v_j \frac{\langle C^2 \rangle}{2}\right)\right] =$$

$$-\tau_{ij}\frac{\partial v_i}{\partial x_j} - \frac{\partial\left(q_j^k + q_j^c\right)}{\partial x_j} - \gamma + \beta\langle C_{gi}C_i - C_iC_i\rangle \qquad \text{Eq.7.6}$$

⟨ ⟩ denotes the ensemble average. The flux of fluctuating kinetic energy, q, is divided into a kinetic and a collisional part. The terms on the right-hand side are in the following order: energy production due to deformation work, energy transfer, γ is the dissipation of energy due to collisions and the last term describes the transfer of fluctuating energy between phases (air and granular phases). This expression can be simplified if the system is assumed to be in local equilibrium. In such a case, the equations simplify to an algebraic expression, thus balancing local production and the dissipation of the fluctuations [van Wachem et.al 2001]. Equation 7.6 is then reduced to Equation 7.7.

$$0 = \left(-\tau_{ij}\frac{\partial v_i}{\partial x_j}\right) - \gamma \qquad \text{Eq.7.7}$$

This assumption has been made in all previous continuum simulations of high-shear granulation and in the attached Papers I and III. The validity of the assumption has been tested in bubbling fluidized beds, with good results, and can, consequently, be believed to be valid for the rapid flow regime.

To be able to solve the full equations expressed above, the fluxes τ_{ij}^{k} and τ_{ij}^{c}, for momentum, and q_j^k and q_j^c plus the rate of dissipation, γ, for the fluctuating velocity are needed. Equation 7.8 is used for energy transfer.

$$q = \kappa\nabla T + \mu_\kappa \nabla\alpha_s \qquad \text{Eq.7.8}$$

Where κ can be seen as the conductivity of the velocity fluctuations or granular temperature. The second term with the coefficient μ_κ is significant only for flows of inelastic particles and is further discussed in Paper VII.

For the momentum transfer, the combined stress tensor can be written in the form of Newton’s Law of Viscosity (Equation 7.9).

$$\tau = \left(\lambda - \frac{2}{3}\mu\right)(\nabla\cdot\mathbf{u})I + 2\mu S \qquad \text{Eq.7.9}$$

Where λ represents the bulk viscosity and μ the shear viscosity.

All the transport coefficients and the dissipation rate can now be written as functions of $f(r_1, v_1, t)$ only. To get a closed system of equations, $f(r_1, v_1, t)$ must be described as a function of the above stated fields (mass, momentum and fluctuating kinetic energy).

7.1.2 The Chapman-Enskog method

The Chapman-Enskog method [Chapman and Cowling 1970] is a way of solving the Boltzmann Equation for systems near equilibrium. The method is based on expansion in a series of powers of $f(r_1, v_1, t)$ around some known solution. This is called a pertubative solution method. The solution used is the equilibrium solution, meaning that it describes a system that is uniform in all fields. The solution is then expanded in a parameter, δ, with a small value and in the gradient of one of the field properties, x, (Equation 7.10).

$$f = f^0(1 + \delta\nabla x + \delta^2\nabla^2 x + \ldots) \qquad \text{Eq.7.10}$$

The number of terms that are taken into account will affect the properties of the model. Retaining only f^0 gives an equilibrium solution represented by a Maxwellian velocity distribution in all positions in the system. First-order expansion is considered in the standard solution. The resulting expressions for the transport coefficient are called the Navier-Stokes order. Many investigations use only Navier-Stokes expressions to derive the transport equations of hydrodynamic fields, and such expressions have proven to provide good agreement for dilute systems near equilibrium[Glasser and Goldhirsch 2001] [Montanero et.al. 1999] [Santos et.al. 1998]. There are alternative ways of carrying out the expansion around an equilibrium solution. The choice of a small parameter and a hydrodynamic field derivative will determine the way in which the solution will deviate from equilibrium. The parameter and the field gradients still need to be small in order for the solution to converge as the number of terms is increased. In the original Chapman-Enskog expansion, the Knudsen number, K, defined as the ratio between the mean free path of the particles and the characteristic length-scale of the flow, is used. This implies that K is small, meaning that there is a separation of scales between the flow of individual particles and the macroscopic flow of the particle phase. For systems of slightly inelastic particles, the so-called inelasticity parameter ϵ, defined as $\epsilon = 1 - e$, is often used [Sela and Goldhirsh 1998]. Both of these modifications will give improved models for use in high shear mixers; however, for modelling they will only give one feature at a time. Sela and Goldhirsh 1998 [Sela and Goldhirsh 1998] made a double expansion in both K and ϵ, and this gave a different dependence of viscosity on ϵ and the number density of particles. The difference was found to be due to this form of expansion which leads to the inclusion of a quasi-microscopic rate of decay in the particle velocity fluctuations that had not been accounted for previously.

Examples of Navier-Stokes order expressions for shear viscosity [Gidaspow et.al. 1992], bulk viscosity [Lun et.al 1984], and dissipation rate [Lun et.al 1984] are shown in Equations 7.11-7.13. The expressions are those used in previous attempts at continuum modelling of high shear granulation as well as in the attached Papers I and III.

$$\mu = \frac{4}{5}\alpha_s^2\rho_s d_p g_0(1+e)\sqrt{\frac{T}{\pi}} + \frac{1}{15}\sqrt{T\pi}\rho_s d_p g_0 \frac{(1+e)(3/2e-1/2)}{(3/2-e/2)}\alpha_s^2 + \frac{1}{12}\frac{\alpha_s\rho_s d_p\sqrt{T\pi}}{(3/2-e/2)} \qquad \text{Eq.7.11}$$

$$\lambda_s = \frac{4}{3}\alpha_s^2\rho_s D_p(1+e)\sqrt{\frac{T}{\pi}} \qquad \text{Eq.7.12}$$

$$\gamma = \frac{12(1-e^2)g_0}{d_p\sqrt{\pi}}\rho_s\alpha_s^2 T^{3/2} \qquad \text{Eq.7.13}$$

where g_0 is the radial distribution function and T is the granular temperature.

Keeping the second-order terms in Equation 7.10 will lead to the so called Burnett Equations [Sela and Goldhirsh 1998] [Brey et.al. 1998]. Sela and Goldhirsh's doubled expansion in K and ϵ was also carried out to the Burnett order. The resulting expressions have proven to resolve some important features of non-equilibrium particle systems in a uniform shear flow. The results show that the equations are able to resolve the anisotropy of fluctuating kinetic energy, something that the Navier-Stokes equations are not capable of. They continue to describe the solution, pointing to the problem that the Burnett order terms are mathematically ill-posed for unstationary problems.

The equilibrium solution, that is the starting term of the expansion, should also be examined in order to improve the model for sheared high solid volume fraction flows of inelastic particles. It is a problem as such to have an equilibrium solution of a system in which energy dissipates through inelastic collisions. The next section will discuss a method for improving the equilibrium solution for high solid volume fraction flows.

7.2 The revised Enskog theory

The Revised Enskog Theory (RET) was developed by Beijeren and Ernst 1979 [Beijeren and Ernst 1979]. The authors developed equations for $f(r_1, v_1, t)$ in systems with hard spheres, similar to the Boltzmann Equation, but used a fractional dependence of f on field variables. This led to a correct description of the system at equilibrium in all states; from gas-like to solid-like.

Hydrodynamic models based on RET, in which the first three statistical moments of $f(r_1, v_1, t)$ are described, were presented by Dufty et.al. 1996 [Dufty et.al. 1996]. The models for the transport coefficients show good agreement for equilibrium systems. The models have also been tested for non-equilibrium [Santos et.al. 1998] systems subjected to uniform shear, and have shown good agreement with DEM simulations. It is possible to predict the qualitative dependence of viscosity on shear rate, with a shear thinning at low shear rates followed by a shear thickening as the rate increases. This RET approach was used by Garzo and Dufty 1999 [Garzo and Dufty 1999], and was expanded to be valid for inelastic spheres.

The RET concept gives a correct description of equilibrium systems to the limit of close packing of spheres. The kinetic equations from this approach have also proven to give good agreement for non-equilibrium systems of uniform shear flows. This approach is able to describe the switch from shear thinning to shear thickening. The use of this model for real non-equilibrium and high solid volume fraction systems still remains questionable since it does not include any effects of long duration contacts or frictional dissipation in the expression for the collision integral.

7.3 The friction model

Shaeffer [Shaeffer 1987] and Johnson and Jackson [Johnson and Jackson 1987] have extended the KTGF approach to account for dense particle flows.

In [Shaeffer 1987] continuum equations for use in, for example, emptying silos are derived. This type of equation is intended to describe the limit of no-flow or flow in the quasi-static regime. The resulting expression for the frictional stresses, $\mu_{s,friction}$, is calculated from Equation 7.14.

$$\mu_{s,friction} = N_f \sin(\varphi) \qquad \text{Eq.7.14}$$

where φ is a frictional parameter of the material, called the angle of internal friction, and N_f is the normal stress. N_f is assumed to rapidly diverge as the volume fraction approaches the maximum packing of the material, according to Equation 7.15.

$$N_f = \frac{Fr}{(\alpha_{max} - \alpha)^n} \qquad \text{Eq.7.15}$$

In Equation 7.15, Fr is a constant determined by curve fitting to the experimental data from the Couette shear cell experiments done in [Savage and Sayed 1984]. The exponent, n, is set equal to 40 [Johnson and Jackson 1987].

The model was validated against experimental data from [Savage and Sayed 1984]. It gives reasonable fits for volume fractions from 0.477 to 0.522.

The assumption that the frictional stress is additive to the other stress contributions, derived from KTGF, was first used in [Johnson and Jackson 1987]. In that paper the authors stress the simplicity of the assumption. The final sentence of the paper says, "... a theory of the present type can only be regarded as an expedient substitute for a proper treatment of particle-particle contact interactions of a dissipative nature, with arbitrary duration.".

7.4 Empirical adaptations to observations

The fact that shear viscosity diverges faster than the transport rate of velocity fluctuations [Bocquet et.al. 2001] has led to the development of models that use the Navier-Stokes hydrodynamic expressions; however, modified in such a way that the discussed property of viscosity is present. The expression used for shear viscosity is shown in Equation 7.16.

$$\mu = \mu_1 \frac{\sqrt{T}}{\left(1 - \alpha_s / \alpha_{s,max}\right)^{\beta}} \qquad \text{Eq.7.16}$$

Where β is the rate-determining exponent and is 2.58 for hard spheres [Barrat et.al. 1989] for the shear viscosity and unity for all other coefficients. This earlier divergence-rate behaviour was also studied by Garcia-Rojo et.al 2006 [Garcia-Rojo et.al 2006], in which those authors used MD simulations to show this relation for elastic hard disks. Khain and Meerson 2006 [Khain and Meerson 2006] have used this relation for modelling the slightly inelastic shear flow of hard spheres. They found that the faster divergence of shear viscosity, in comparison to other transport coefficients, allows for the existence of liquid-like and solid-like regions when sheared high solid volume fraction flows are studied. The expression they used is shown in Equation 7.17.

$$\mu = \mu_1 \frac{\alpha_{s,max}\sqrt{T}}{(\alpha^*_{s,max} - \alpha_s)d^2} \qquad \text{Eq.7.17}$$

Where $\alpha^*_{s,max}$ is smaller than $\alpha_{s,max}$. The other transport coefficients all diverge at the rate of $\left(\alpha_{s,max} - \alpha_s\right)^{-1}$. These types of adaptions to experimental observations, or DEM simulation, presented here, result in qualitative agreement in the behaviour of flows with solid-like and fluid-like regions approaching close packing. The method is somewhat empirical, and there is a question about the generality of the results in predicting the point of transition in a flow from a fluid-like to a solid-like behaviour.

7.5 The Rheology model

The model, here called the rheology model, was proposed by Jop et al. in [Jop et al., 2006]. The model is based on a functional expression found through observations of hopper flows and particle flows on slides. The model is specifically devised for dense granular flows, and even includes the assumption of a constant solid volume fraction. Shear stresses are formulated as a function of isentropic pressure and a complex friction coefficient, μ, in Equation 7.18.

$$\tau = \mu(I)P \qquad \text{Eq.7.18}$$

The friction coefficient is defined in Equation 7.19, and it is a function fitted to an experimentally found behaviour of the coefficient.

$$\mu(I) = \mu_s + \frac{(\mu_a - \mu_s)}{\left(I_0 / I + 1\right)} \qquad \text{Eq.7.19}$$

The subscript indexes in μ_s and μ_a represent start and stop. This means that they are either the values taken or the friction coefficient at the angle at which flow starts down an inclined plane and the value at which flow stops if already in progress. The function interpolates between the values of μ_s and μ_a through a functional dependence on I which is a dimensionless number called the inertial number, Equation 7.20.

$$I = \gamma \frac{d}{\left(P/\rho\right)^{0.5}} \qquad \text{Eq.7.20}$$

where d is the particle size, ρ is the particle density, γ is the shear rate and P is the isentropic pressure. The inertial number relates the shear forces in the material to the normal forces due to isentropic pressure. This gives a measure of the likelihood of a particle to move out of its lattice-like cage of surrounding particles, or a relation between the time scale of the rearrangement of particles (t_{micro}) to the time scale of the translation of the bulk (t_{macro}). It can be used as a flow regime indicator [da Cruz et al. 2005] in which large values of I mean relatively large shear, and a high degree of rearrangements among the particles giving a more rapid system while higher confining pressures leads to that bulk motion is dominant with solid like behaviour. In [Pouliquen et.al. 2006] Pouliquen et.al. show that $I = 0.3$ defines the switch point at which the rheology model is no longer valid. For the particles used here, a direct relation can be found to the solid volume fraction, thus giving a value of 0.5-0.55 [Pouliquen et.al. 2006].

I_0 is a constant related to the particle properties, defined according to Equation 7.21.

$$I_0 = \frac{5}{2}\frac{d\beta}{L_0\sqrt{\phi\cos(\theta)}} \qquad \text{Eq.7.21}$$

where d is the diameter of the particle, β and L_0 are constants that are experimentally found [Hatano, 2007] [Jop et al. 2005], ϕ is the volume fraction of solids, θ is an average value for the angle of the inclined surface.

The model expression can also be rearranged to describe an effective viscosity according to Equation 7.22.

$$\eta(|\gamma|,P) = \mu(I)\frac{P}{|\gamma|} \qquad \text{Eq.7.22}$$

This shows an inverse relation to the shear rate and a direct relation to the pressure. This means that viscosity diverges at low shear rates, thus giving a solid like behaviour and a yield criterion according to Equation 7.23.

$$|\tau| > \mu_s P where |\tau| = (0.5\tau_{ij}\tau_{ij})^{0.5} \qquad \text{Eq.7.23}$$

The material used in the attached Papers II and IV were 1.3mm glass beads. The material data for these particles were taken from Pouliquen 1999 [Pouliquen, 1999].

8. Connecting flow information to the evolution of particle properties (Papers I and VI)

The evolution of particle properties is commonly modelled with population balance equations. The choice of what properties to follow is not only determined by the information of interest in the final product, but also an important choice because of the properties that affect the flow conditions in a vessel. Darelius et.al. [Darelius et.al. 2007] experimentally determined the evolution of a number of bulk properties of a granulate during granulation. In Paper I this information is used to investigate the parameterization of the KTGF framework. The development of mechanistic kernels also shows the importance of keeping track of the internal properties of granules in order to use time-resolved meso-scale flow information. In [Ramachandran et.al. 2009] and [Liu et.al. 2000] aggregation and breakage properties are related to the internal strengths of granules, strengths which can be attributed to the liquid content and compaction of the aggregates. This implies that the use of flow information from a continuum simulation is strongly related to the choice of properties that are monitored and modelled, and the choice of mechanisms and kernels that affect those properties. In this thesis, a first trial to couple a CFD solution to a PBM solver was made. In this trial a relatively simple two-dimensional PBM model was used in which the properties of granular solid and liquid mass were modelled according to Equation 8.1.

$$\frac{V_i \partial n_i(m_s,m_l,t)}{\partial t} = V_i B_0^0 B(m_s,m_l) + V_i R_w^0 R_w(m_s,m_l) + V_i G_0 \frac{\partial n_i(m_s,m_l,t) G(m_s,m_l,t)}{\partial m_s} + \frac{1}{2} V_i \beta_0 \int_0^{m_s} \int_0^{m_l} \beta(m_s,m_l,m'_s,m'_l)\, n_i(m_s - m'_s, m_l - m'_l, t) n_i(m'_s,m'_l,t) dm_s dm_l - V_i \beta_0 n(m_s,m_l,t) \int_0^{\infty} \int_0^{\infty} \beta(m_s,m_l,m'_s,m'_l)\, n_i(m'_s,m'_l,t) dm'_s dm'_l + \sum_{j=1,j\neq i}^{k} \frac{Q_{i\to j}}{V_i} n_i(m_s,m_l,t) + \sum_{j=1,j\neq i}^{k} \frac{Q_{j\to i}}{V_j} n_j(m_s,m_l,t) \qquad \text{Eq.8.1}$$

where $\boldsymbol{m_s}, \boldsymbol{m_l}$are the mass in kg of solid and liquid, respectively, in a granule, V is the compartment volume in m^3 and Q is the flow rate to and from compartments in $\frac{\boldsymbol{m^3}}{\boldsymbol{s}}$. n is the density function, $\frac{\boldsymbol{number\ of\ particles}}{\boldsymbol{kg^2 m^3}}$. G, B, R and β are layering, nucleation, rewetting and aggregation, respectively, which are the mechanisms used.

The aggregation kernel used was that by Tan et al [Tan et.al. 2004]. The derivation of the aggregation kernel is based on the principles of the kinetic theory of granular flow (KTGF) and the Equipartition of Kinetic Energy Kernel (EKE) developed by Hounslow [Hounslow 1998]. The aggregation kernel can be seen in Equation 8.2 below

$$\beta_{i,j} = \psi g_{i,j} \sqrt{\frac{3\theta_s}{\rho}} \left(l_i + l_j\right)^2 \sqrt{\frac{1}{l_i^3} + \frac{1}{l_j^3}} \qquad \text{Eq.8.2}$$

where ψ is the aggregation efficiency, θ_s is the mixture granular temperature which is similar to the description of granular temperature in KTGF, Equation 8.3.

$$\theta_s = \frac{1}{3} m_n \langle C \cdot C \rangle = m_n \theta \qquad \text{Eq.8.3}$$

where m_n is the average mass of a particle and C is the random fluctuating part of the decomposed actual particle velocity from the KTGF. The aggregation kernel consists of one size-dependent part, which is the EKE kernel, Equation 8.4.

$$\beta(l_i, l_j) = (l_i + l_j)^2 \sqrt{\frac{1}{l_i^3} + \frac{1}{l_j^3}} \qquad \text{Eq.8.4}$$

and a time-dependent part, Equation 8.5.

$$\beta_0(t) = \psi g_0 \sqrt{\frac{3\theta_s}{\rho}} \qquad \text{Eq.8.5}$$

where l is particle size, g_0 the radial distribution function of the particle volume fraction defined as in Equation 8.6.

$$g_0 = \left[1 - \left(\frac{\alpha_s}{\alpha_{s,max}}\right)^{1/3}\right]^{-1} \qquad \text{Eq.8.6}$$

Of special interest is the time-dependent part of the aggregation kernel, Equation 8.6, which will be calculated from CFD simulations rather than found experimentally. Benefits from actually calculating this is not only that no experiments for the specific granulator are needed, but it is also a way to estimate the actual rate of aggregation locally in the system.

9. Results and discussion

This section contains summaries of the results in attached papers. All of the papers address continuum modelling of granular flows in high shear mixers. Papers I and VI use the KTGF + friction continuum model to study its parametrization and the change in granular properties as the granulation progresses. Paper II shows the impact of the resolution dependence of the KTGF + friction model while Papers III, IV, V and VII introduce improved approaches for modelling dense sheared flows in high shear mixers.

9.1 Parameterization and connection to PBM (Papers I and VI)

Paper I investigates the parameterization of the KTGF models, considering particle properties and the ability of the model to resolve property changes during a granulation process. The parameters in the model that were chosen for the study were: the angle of internal friction (φ), the restitution coefficient (e), the particle diameter (d_p), the particle density (ρ_s), the packing limit and the granular phase velocity wall boundary condition (slip condition). These are the parameters that characterize the powder or granules used in the simulation. Changes in these parameters can be seen as a comparison of the use of different materials. These parameters are also expected to change during granulation [Darelius et.al. 2007]. The parameter settings for the base case and variations are given in Table 9.1.

Table 9.1. The parameter settings for the base case (0) and the variations (+,-).

Parameter	-	0	+
Particle Velocity B.C.	0.01	10	No slip
d_p	0.855mm	1.355mm	1.855mm
φ	28^o	38^o	48^o
E	0.46	0.9	0.99
ρ_s	2000kg/m^3	2700kg/m^3	3400kg/m^3
Frictional Packing limit	0.45	0.5	0.55
Packing limit	-	0.63	0.68

The study shows that both the KTGF part and the frictional model are important for the solution. This can be seen by the influence of parameters only present in the KTGF model (e and d_p) as well as an influence of the frictional parameter φ. This indicates that the flow is a mixture of quasi-static and rapid flow. Only a change in the boundary conditions for granular phase velocity, from partial slip to no slip, fundamentally changes the flow. This is shown in Figure 9.1 where it can be seen that the extra energy input from the impeller has dispersed the flow.

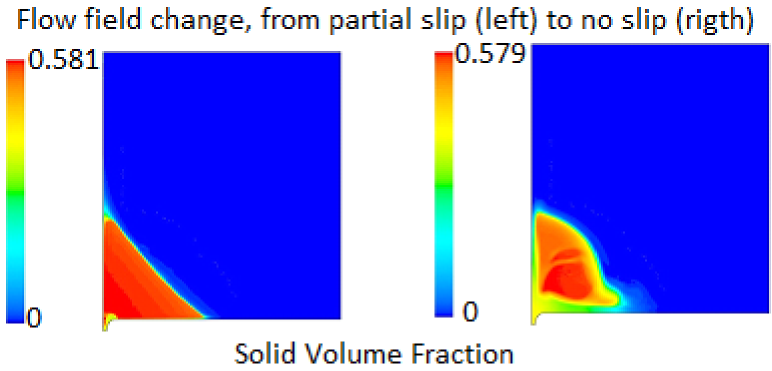

Figure 9.1. The change in solid volume fraction in the flow when changing from a partial slip to a no slip boundary condition.

The most important particle parameters were, therefore, concluded to be e and φ. The model is sensitive to changes in e in the region of validity for the KTGF model, close to elastic collisions. φ is the determining parameter in the frictional model, and its importance proves the influence of the frictional model.

A test was made to investigate if the parameterization of the model is able to predict the increase in impeller torque that is normally seen when going from the dry powder mixing stage to the wet massing stage [Leuenberger 1982]. The test result showed that the model can predict the change in impeller torque, and that the adhesion of the powder to the vessel walls and impeller is the most important factor causing this increase.

After investigating the parameterization of the KTGF model and its possible use for feeding a PBM solver with flow field information, the question remained how to couple the two modelling approaches. In manuscript VI a coupled continuum CFD simulation and PBM solver were used to analyse meso-scale properties in the flow field. The connection was made with a compartment model in which properties and fluxes between compartments were extracted from the CFD solution. The compartment approach was based on the aggregation rate in the compartments, which is a function of granular temperature and volume fraction, and showed that separate regions could be found; for example, a high aggregation compartment was found at the impeller blade, shown in Figure 9.2 (left). Figure 9.2 (right) also shows the distribution of experienced aggregation rates over the mass of the granules in the vessel. For the three CFD cases this represents an evolution in time.

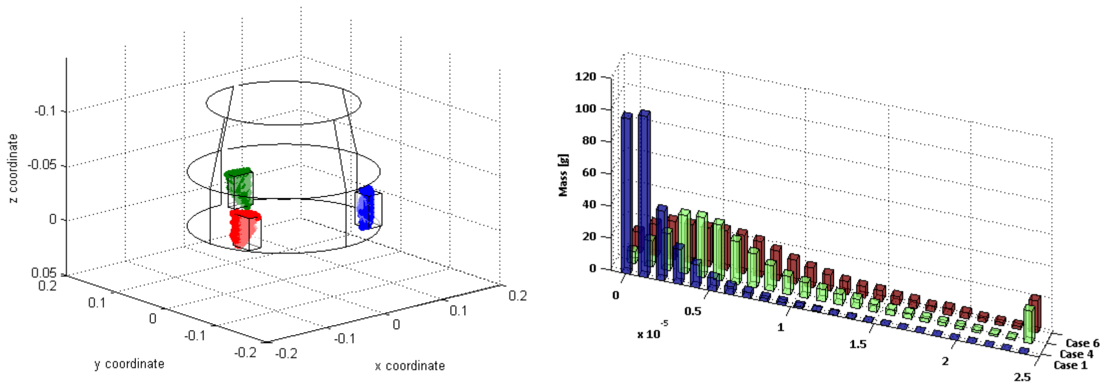

Figure 9.2. Impeller compartments separated based on aggregation rate (β_0). Coordinate axes are distance in meters (left) and the particle mass distribution of β_0 in the vessel for three flow cases representing temporal changes during a granulation.

The high fluxes between the compartments prevented the spatial compartmentalization from having any effect on the PBM solution for this case. The temporal changes seen in Figure 9.2 (right) led to changes in the overall average aggregation rate, the values of which are presented in Table 9.2.

Table 9.2. Averages aggregation rate values for the three flow cases.

Case	**1**	**4**	**6**
$\beta_0 \times 10^6$	0.65	3.12	3.06

It is believed that for a more elaborate set of mechanisms, in which thresholds for breakage or memory effects from compaction are included, the spatial compartment analysis would also be of importance.

9.2 Evaluation of the KTGF + friction framework (Paper III)

One of the assumed reasons for the deficiencies found in [Darelius et.al. 2008] and Ng et.al. 2009] was the mesh resolution close to the walls. No study of the mesh dependence of the solution was done in [Darelius et.al. 2008]. Only a global mesh refinement was made in [Ng et.al. 2009], and those authors only examined changes in global flow. This same procedure was used in the attached Paper I, but with the conclusion that a much finer mesh was needed, in respect to particle size, than in both [Darelius et.al. 2008] and [Ng et.al. 2009] in order to obtain only a small change in solid viscosity. It is also important to investigate the effect of the lack of separation of scales on the solution by investigating what happens as the mesh size goes towards particle size. It was, therefore, decided to investigate the effects of spatial resolution on the KTGF + friction framework.

The system studied was a Couette shear cell, which consisted of two concentric cylinders with a gap in between in which an inner cylinder rotates. The study was done by gradually increasing the resolution, and investigating the velocity profile and comparing it to literature data, profiles of the frictional contribution to the solid viscosity, here called frictional viscosity, the ratio of frictional viscosity to the collisional and translational contributions, and the solid volume fraction. The results are shown in Figure 9.3.

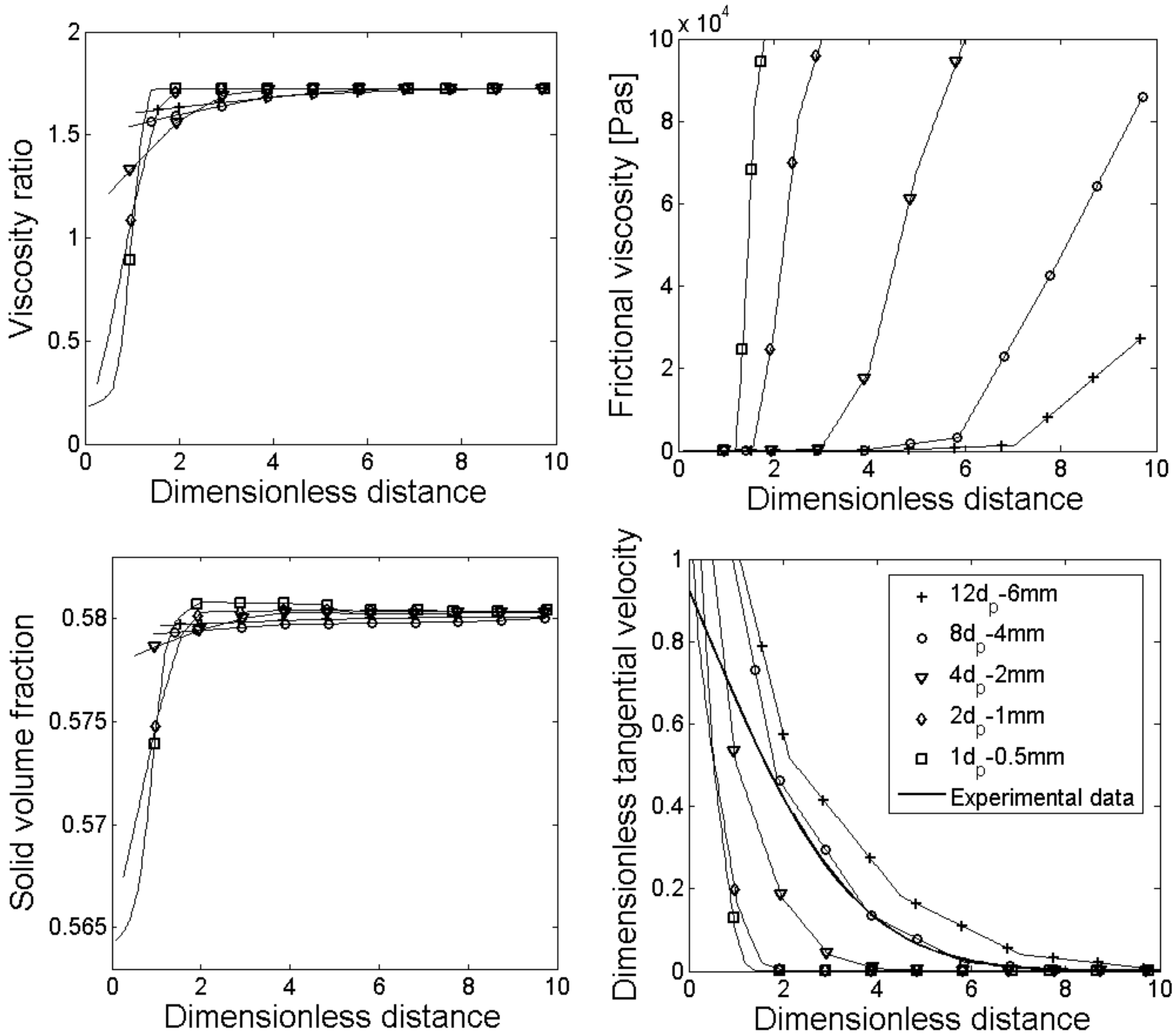

Figure 9.3.Top left: viscosity ratio profiles, top right: frictional viscosity profiles, bottom left: solid volume fraction profiles and bottom right: dimensionless tangential velocity profiles. The dimensionless distance from the inner wall is plotted on the x axis for the figures defined as distance divided by the particle diameter. The same legend is used for all four figures.

Figure 9.3 shows clearly that the lack of separation of scales in granular flows affects both the distribution and the magnitude of the solid phase stresses. The change is towards an increase in the importance of frictional stresses and towards a general increase in solid viscosity as the resolution is improved. The results show that the KTGF + friction framework is resolution-dependent down to the particle length-scale. When these results were related to the simulations of high shear granulation equipment [Darelius et.al. 2008, Ng et.al. 2009], it was concluded that an underestimated viscosity in the near wall region also needed to be analysed in the perspective of spatial resolution in relation to particle size.

9.3 Modifications of the KTGF equations for dense granular flows (Papers II, IV, V and VII)

Two approaches to modifications of the KTGF equations were made in this research to try to improve the predictions for dense, inelastic sheared flows. The near-wall and impeller regions in a high shear granulator are non-equilibrium regions (large gradients in both volume fraction and velocity) with densely packed inelastic particles. Such a system is not well modelled by the traditional KTGF equation, and the added frictional model does not give adequate predictions. There are existing derivations of KTGF equations in which the assumptions behind the original theory are relaxed in order to better describe denser systems or systems farther from equilibrium.

In [Bouquet et.al. 2001] it was found in Couette cell experiments that shear viscosity diverges faster than other transport coefficients. This has proven important in modelling the transition between the solid-like and fluid-like behaviour of a flow. In [Khain and Meerson 2006] this was used to develop a model for dense granular flow that was able to predict the fluid-like to solid-like transition for a uniform shear flow of slightly inelastic particles. The model in that article was an adaptation of experimental findings or DEM models, and, for that reason, it would be preferable to achieve the same behaviour in a rigorous way. In Paper V, a study using this approach was conducted at high solid volume fraction and under shear. Comparisons were made between KTGF, KTGF + friction and viscosity divergence approaches. Figure 9.4 shows experimental and model predicted values of stress strain relations.

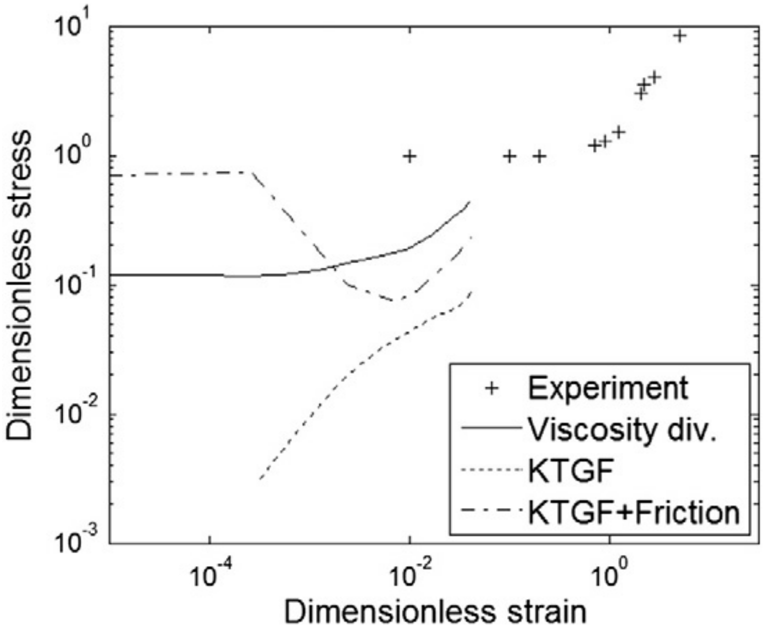

Figure 9.4. The stress strain relation for the models used in Paper V.

Figure 9.4 shows that the viscosity divergence model can qualitatively match the behaviour of the experimental data found in the literature, in contrast to the KTGF+Friction and the pure KTGF models.

The results of Paper V were considered to demonstrate that the viscosity divergence model contains an important feature for the volume fraction dependence of the transport coefficients in dense granular flows. This was an experimentally found relation, and, in Paper VII, it was combined with the theoretical framework of the RET. The RET version used was the one derived in Garzo et.al. [Garzo et.al. 1999] for inelastic particles at all densities at equilibrium. The idea was to introduce viscosity divergence volume fraction dependence through the radial distribution function. The reason for introducing this was to improve the predictions for dense non-equilibrium systems by introducing an experimentally found property in which effects such as long duration contacts and frictional sliding are present. The results showed that there were improvements when the viscosity divergence distribution function was used. Figure 9.5 shows the velocity and granular temperature profiles of the models evaluated.

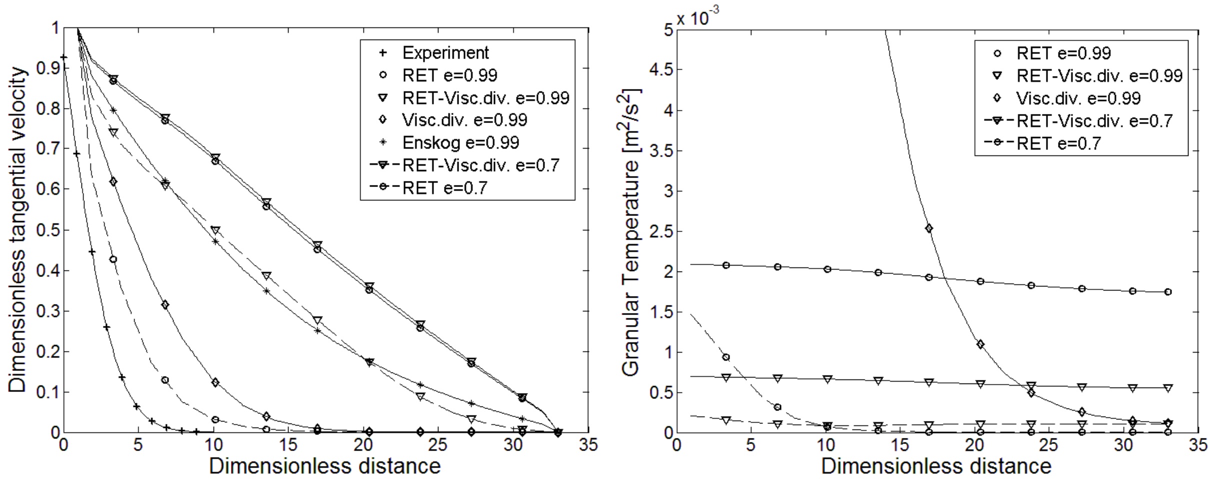

Figure 9.5. Velocity profiles (left) and granular temperature profiles (right).

However, the new model failed to predict the phase transition and the change in the stress strain relation which accompanied that. This is shown in Figure 9.6.

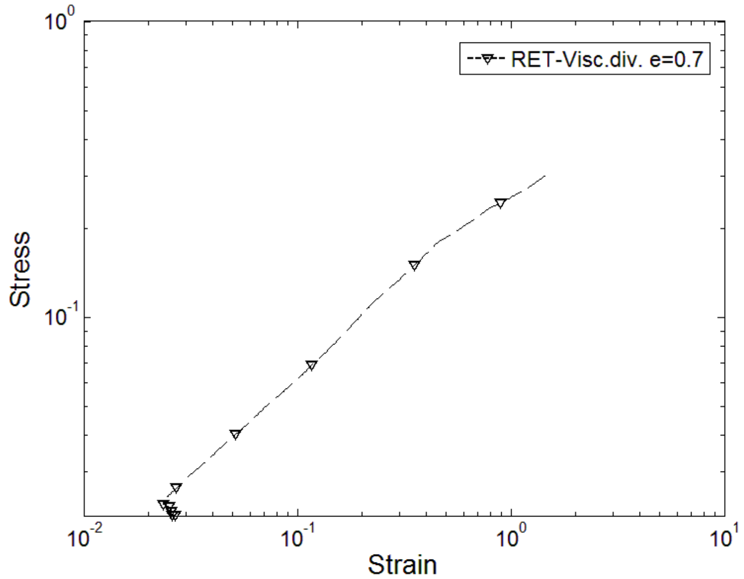

Figure 9.6. Stress strain relation for the new model with e = 0.7.

The reason for the inability of the model to make the same predictions as in Paper V is that the inelasticity of the system led to a large drop in granular temperature over the annulus, as seen in Figure 9.5 (right). Since viscosity is related to granular temperature, it will remain low despite the divergence caused by the high volume fraction. It was concluded that this set of transport coefficients are best suited for dilute to intermediate granular flows.

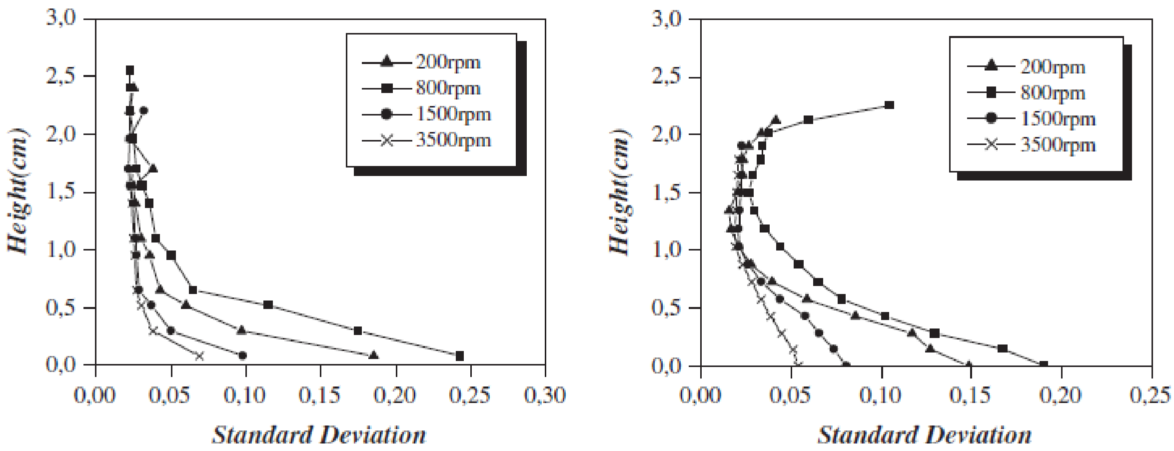

Figure 9.7. Profiles of the standard deviation of instantaneous velocity, experimental data (left) and model predictions (right).

In Papers II and IV an approach to handling dense granular flows different to the one in the KTGF model was evaluated and developed for use in HSG equipment. The models were based on Jop et.al. [Jop et.al. 2006]. In Paper II the model was used in a disc impeller granulator with the assumption of a constant volume fraction in the system. The left graph in Figure 9.7 shows the experimentally obtained values of the velocity standard deviation. The figure indicates that the system was diluted by the random motion of the particles. An interesting secondary observation was that the excitation of the system was not proportional to impeller velocity. Instead, it showed a maximum excitation at 800 rpm which then decreased at 1500 and 3000 rpm. This shows that the velocity boundary condition is of great importance, and, for this reason, a torque-fitted partial slip expression was used as described in Paper II. The velocity predictions by the model used in Paper II gave indications that the model can give improved predictions for dense granular flows, Figure 9.8 (bottom right). The model needs to be connected with a model for the dilute parts, like a KTGF model, in order to redistribute some of the tangential velocity to random particle motion and to resolve the volume fraction changes near the impeller.

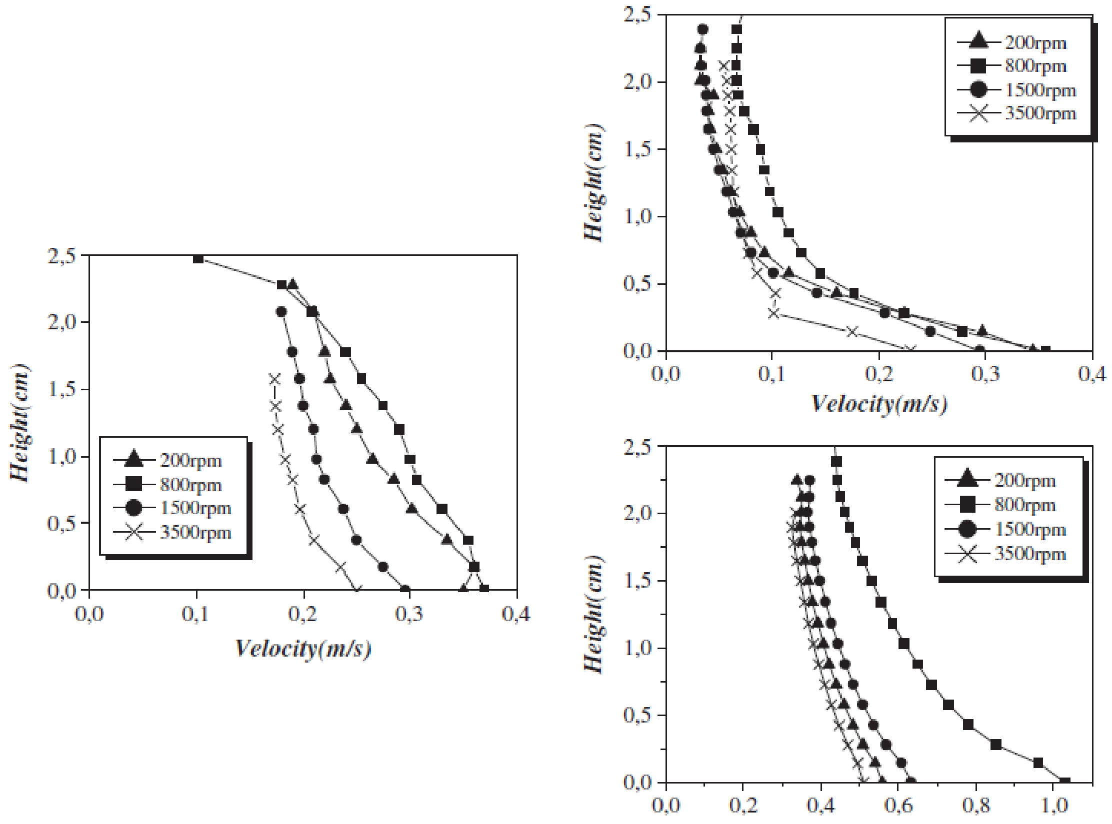

Figure 9.8. Velocity profiles comparing experimental data (left) to the Rheology model (bottom right) and Rheology + KTGF model (top right) predictions.

Figure 9.8 shows that the rheology approach has great potential to model dense parts of an HSG. The use of the switch criterion to a KTGF-type of model also worked well and showed that this approach has potential. However, the conclusion was that the standard KTGF model used was not adequate for the moderate volume fractions around the switch value. This led to the conclusion that a combination of model approaches tested here; a RET viscosity divergence model and a Rheology model, has the potential to give further improved model predictions. This notion has not yet been tested, and will be included in future research.

10. Conclusions

Several approaches to modelling were tested and evaluated for use with HSG equipment. The KTGF+friction approach was not good enough because of its resolution dependence, and it was also found to give qualitatively wrong predictions for the stress strain relations in a Couette cell. Several models with improved predictions were suggested: a viscosity divergence approach, and a RET and Rheology model. These models have shown improved predictions on their own, but the most promising approach would be a combination. The KTGF combined Rheology model showed better prediction abilities. In combination with the RET, this model is believed to give even further improvements.

The parameterization of this model framework seemed, at a first trial, to be able to describe a granulation process. The boundary condition is the most important factor for capturing the changes in impeller torque as granulation progresses. A compartment approach connected to a PBM solver of desired particle properties was also developed and showed promising potential to give meso-scale information. This is useful in the evaluation of new equipment designs and in up-scaling to full-scale production.

11. Future work

Final steps are needed to conclude the work of continuum modelling for HSG equipment. The full combination of possible models still remains to be tested in different equipment and validated with experimental data. The continuum model needs to be incorporated into the compartment model and tested with different PBM approaches, in order to examine the effects of a flow field on the properties and mechanisms of granules such as compaction, hardness and mechanistic breakage.

References

Agrawal K., Loezos P. N., Syamlal M., Sundaresan S., 2001. The role of meso-scale structures in rapid gas-solid flows, JOURNAL OF FLUID MECHANICS, 445, 151-185.

Bagnold R.A. 1954. Experiments on a gravity-free dispersion of large solid spheres in a Newtonian fluid under shear, Proceedings of the Royal Society of London / A, 225, 1160, 49-63

Barrat J.L., Goetze W., Latz A., 1989. The liquid–glass transition of the hard-sphere system, J. Phys. Condens. Matter, 1, 7163–7170.

Bocquet L., Losert L., Schalk W., Lubensky T.C., Gollub J.P., 2001. Granular shear flow dynamics and forces: Experiment and continuum theory, Phys. Rev. E, 65, 011307.

Brey J. J., Dufty J. W., Kim C. S., Santos A., 1998. Hydrodynamics for granular flow at low density, Phys. Rev. E, 58, 4, 4638-4653.

Chapman S. and Cowling T.G., 1970. The mathematical theory of non-uniform gases, Cambridge university press, third edition.

Coulomb C.A., 1776. Essai sur une application des règles de maximis et minimis à quelques problèmes de statique, relatifs à l'aarchitecture, Mèmoires de l'Academie Royale Pres Divers Savants 7, 343-382.

da Cruz F., Emam S., Prochnow M., Roux J.-N., Chevoir F., 2005, Rheophysics of dense granular materials: discrete simulation of plane shear flows, Phys. Rev. E. 72, 021309.

Darelius A., Brage H., Rasmuson A., Niklasson Björn I., Folestad S., 2006. A Volume-based multi-dimensional population balance approach for modelling high shear granulation, Chem. Eng. Sci. 61, 2482-2493.

Darelius A., Lennartsson E., Rasmuson A., Niklasson Björn I., Folestad S., 2007. Measurement of velocity field and frictional properties of wet masses in a high shear mixer, Chem. Eng. Sci. 62, 2366-2374.

Dufty J. W., Santos A., Brey J. J., 1996. Practical Kinetic Model for Hard Sphere Dynamics, Phys. Rev. Lett., 77, 7, 1270-1273

Enwald H., Peirano E. and Almstedt A.-E., 1996. Eulerian two-phase flow theory applied to fluidization. Int. J. Multiphase Flow, 22, 21-66.

Darelius A., Rasmuson A., van Wachem B., Niklasson Björn I., Folestad S., 2008. CFD simulation of the high shear mixing process using kinetic theory of granular flow and frictional stress models, Chem. Eng. Sci. 63, 2188-2197.

Forterre Y., Pouliquen O., 2003. Long-surface-wave instability in dense granular flows, J.Fluid Mech. 486, 21–50.

Gantt J.A., Cameron I.T., Litster J.D., Gatzke E.P., 2006a. Determination of coalescence kernels for high-shear granulation using DEM simulations, Powder Technol. 170, 53-63.

Gantt J.A., Gatzke E.P., 2006b. Kinetic theory of granular flow limitations for modelling high-shear mixing. Ind. Eng. Chem. Res., 45, 6721-6727

Garcia-Rojo R., Luding S., Brey J. J., 2006. Transport coefficients for dense hard-disk systems, Phys. Rev. E, 74, 6, 061305-1-11.

Garzo V., Dufty J. W., 1999. Dense fluid transport for inelastic hard spheres. Phys. Rev. E, 59, 5, 5895-5911.

GDR MiDi, 2004, On dense granular flows. Eur. Phys. J. E 14, 341-365.

Gidaspow, D., Bezburuah, R., Ding, J., 1992. Hydrodynamics of circulating fluidized beds, kinetic theory approach. In: Fluidization, vol. VII, Proceedings of the 7th Engineering Foundation Conference on Fluidization, Brisbane, Australia, pp. 75–82.

Glasser B.J., Goldhirsch I.,2001. Scale dependence, correlations, and fluctuations of stresses in rapid granular flows, Physics of fluids 13, 2, 407-420.

Hatano, T., 2007. Rheology of a dense granular material. J. Phys. Conf. Ser. 89, 12–15.

Hounslow M.J., 1998, The population balance as a tool for understanding particle rate processes, Kona, 179–193.

Hounslow M.J., Pearson J.M.K., Instone T., 2001. Tracer Studies of High-Shear Granulation: II. Population Balance Modeling, AIChE J. 41, 9, 1984-1999.

Hsiau S., Shieh Y., 2000. Effect of solid fraction on fluctuations and self-diffusion of sheared granular flows, Chem. Eng. Sci. 55, 1969-1979.

Iveson S.M., Litster J. D., Hapgood K, Ennis B.J., 2001. Nucleation, growth and breakage phenomena in agitated wet granulation processes: a review, Powder Technol. 117, 3-39.

Jeans Sir J., 1962. An introduction to the Kinetic Theory of Gases. The syndics of the Cambridge university press, first edition reprint.

Johnson P.C., Jackson R., 1987. Frictional collinsional constitutive relations for granular materials, with application to plane shearing, J. Fluid Mechanics 176, 67-93.

Jop P., Forterre Y., Pouliquen O., 2005. Crucial role of sidewalls in granular surface flows: consequences for the rheology, J. Fluid Mech. 541, 167.

Jop P., Forterre Y., Pouliquen O., 2006. A constitutive law for dense granular flows, Nature, 441, 727–730.

Ketterhagen W.R., Am Ende M.T., Han cock B.C., 2009. Process Modeling in the Pharmaceutical Industry 1using the Discrete Element Method, Journal of Pharmaceutical Science 98, 442-470.

Khain E. and Meerson B., 2006. Shear-induced crystallization of dense rapid granular flow: Hydrodynamics beyond the melting point, Phys. Rev. E, 73 061301-1-11.

Knight P.C., Seville J.P.K., Wellm A.B., Instone T., 2001. Prediction of impeller torque in high shear powder mixers. Chem. Eng. Sci. 56 4457-4471.

Leuenberger H., 1982. Granulation, New Techniques, Pharm. Acta. Helv. 57, 3, 72-82.

Liu L. X., Litster J. D., Associates G., Road H. H., 2000, Coalescence of Deformable Granules in Wet Granulation Processes, vol. 46, no. 3, pp. 529–539.

Luding S., 2009. Towards dense, realistic granular media in 2D, NONLINEARITY, 22, 12, R101-R146.

Lun C.K.K., Savage S.B., Jeffrey D.J., Chepurneiy N., 1984. Kinetic theories for granular flow: inelastic particles in Couette flows and slightly inelastic particles in general flow field, J. Fluid Mechanics 140, 223-256.

McDougall S., Oldrich H., 2004. A model for the analysis of rapid landslide motion across three-dimensional terrain, Can. Geotech. J., 41, 1084-1097.

Mitrano P., Zenk J. R., Benyahia S., Galvin J. E., Dahl S. R., Hrenya C. M., 2014. Kinetic-theory predictions of clustering instabilities in granular flows: beyond the small-Knudsen-number regime. JOURNAL OF FLUID MECHANICS, 738, R2.

Montanero M., Garzo V., Santos A., Brey J. J., 1999. Kinetic theory of simple granular shear flows of smooth hard spheres. J. Fluid Mech. 391-411.

Mueth D.M. 2003. Measurment of particle dynamics in slow, dense granular Couette flow, Physical Review E 67, 011304.

Ng B.H., Kwan C.C., Ding Y.L., Ghadiri M., Fan X.F., 2007. Solid motion in a conical frustum-shaped high shear mixer granulator, Chem. Eng. Sci. 62 756-765.

Ng B.H., Ding Y.L., Ghadiri M., 2009. Modelling of dense and complex granular flow in high shear mixer granulators-A CFD approach, Chem. Eng. Sci. 64, 3622-3632.

Niklasson Björn I., Jansson A., Karlsson M., Folestad S., Rasmuson A., 2005. Empirical to mechanistic modelling in high shear granulation, Chem. Eng. Sci. 60, 3795-3803.

Passalacqua A., Marmo L., 2009. A critical comparison of frictional stress models applied to the simulation of bubbling fluidized beds, Chem. Eng. Sci. 160, 2795-2806.

Pouliquen O., Scaling laws in granular flows down rough inclined planes, Phys. Fluids 11 (1999) 542–548.

Pouliquen O., Cassar C., Jop P., Forterre Y., Nicolas M., 2006 Flow of dense granular material:towards simple constitutive laws, J. Stat. Mech. Theory Exp. P07020.

Ramachandran, R., C. D. Immanuel, et al. 2009. A mechanistic model for granule breakage in population balances of granulation: theoretical kernel development and experimental validation, Chemical Engineering Research and Design 87: 598-614

Remy B., Canty T.M., Khinast J.G., Glasser B. J., 2010, Experiments and simulations of cohesionless particles with varying roughness in a blade mixer, Chem. Eng. Sci. 65 , 4557-4571.

Reynolds G.K., Nilpawar A.M., Salman A.D., Hounslow M.J., 2008. Direct measurement of surface granular temperature in a high shear granulator. Powder Technology, 182, 211-217

Santos A., Montanero J. M., Dufty J. W., Brey J. J., 1998. Kinetic model for the hard-sphere fluid and solid. Phys. Rev. E, 57, 2, 1644-1660.

Savage S.B. and Sayed M., 1984. Stress development by dry cohesionless granular material sheared in an annular shear cell, J- Fluis Mech., 142, 391-430.

Schaeffer D.G., 1987. Instability in the Evolution Equations Describing Incompressible Granular Flow, Journal of Differential Equations 66, 19-50.

Sela N. and Goldhirsch I., 1998. Hydrodynamic equations for rapid flows of smooth inelastic spheres, to Burnett order. J. Fluid Mech., 361, 41-74.

Tan H. S., Goldschmidt M. J. V., Boerefijn R., Hounslow M. J., Salman A. D., Kuipers J. A. M., 2004, Building population balance model for fluidized bed melt granulation: lessons from kinetic theory of granular flow, Powder Technol., vol. 142, no. 2–3, pp. 103–109.

van Beijeren H. and Ernst M.H., 1979. Kinetic Theory of Hard Spheres, J. Stat. Phys., 21, 2, 125-167.

van Wachem B.G.M., Schouten J.C., Krishna R., van den Bleek C.M., 1998. Eulerian Simulation of Bubbling Behaviour in Gas-Solid Fluidised Beds, Computer chem. Engng. 22, 299-306.

van Wachem B.G.M., Schouten J.C., Krishna R., van den Bleek C.M., 1999. Validation of the Eulerian simulated dynamic behaviour of gas-solid fluidised beds, Chem. Eng. Sci. 54, 2141-2149.

van Wachem B.G.M., Schouten J.C., van den Bleek C.M., Krishna R., Sinclair J.L., 2001. Comparative Analysis of CFD Models of Dens Gas-Solid Systems, AIChE J. 47, 5, 1035-1051.